The Journal of Energy: Engineering & Management
Vol. 11, No. 4, Winter 2022, P. 2-9
Research Article

[DOR: 20.1001.1.23452951.1400.11.4.1.0]
[DOI: 10.22052.11.4.2]

Energy Optimization of Under-actuated Crane Model for Time-Variant Load Transferring Using Optimized Adaptive Combined Hierarchical Sliding Mode Controller

Marzieh Ahmadi[1], Alireza Faraji[2*]

[1] Department of Electrical and Computer Engineering, University of Kashan, Kashan, Iran
miss.marziehahmadi@yahoo.com
[2] Department of Electrical and Computer Engineering, University of Kashan, Kashan, Iran
arfaraji@kashanu.ac.ir

Received: 06/23/2020 **Accepted:** 12/20/2021

Abstract
This paper designs an Optimized Adaptive Combined Hierarchical Sliding Mode Controller (OACHSMC) for a time-varying crane model in presence of uncertainties. Uncertainties have always been one of the most important challenges in designing control systems, which include unknown parameters or un-modeled dynamics in systems. Sliding mode controller (SMC) is able to compensate the system in the presence of uncertainties due to un-modeled dynamics and is used for robust stability and performance behavior in the presence of additive un-modeled dynamics of system and multiplicative friction forces. This under-actuated crane has two sub-systems: trolley and payload. Therefore, it can be controlled by a single input signal with combined hierarchical sliding mode controller (CHSMC) using a two-layer-sliding manifold accurately. Payload mass and cable length are time-variant variables through load transferring. Due to the Time-varying models and the inefficiency of most controllers, the use of an adaptive controller can help improve system performance. This controller is adapted by considering a time-varying coefficient of the second layer sliding manifold. For energy saving of the input signal, the parameter of the first layer sliding manifold of ACHSMC is optimized by two intelligent strategies: genetic algorithm (GA) and particle swarm optimization (PSO) method. The simulation results show robust stability and performance of the proposed optimized controller.

Keywords: Time-varying crane model, Uncertainty modelling, Adaptive Control, Combined Hierarchical Sliding Mode Control, Genetic algorithm, Particle Swarm Optimization.

* Corresponding author

[DOR: 20.1001.1.23452951.1400.11.4.1.0]

[DOI: 10.22052.11.4.2]

1. Introduction

In recent decades, a plenty of efforts have been made to control the under-actuated nonlinear systems such as crane system [1], inertia-wheel pendulum [2-4] and so on. [5]. Also, fuzzy method has been applied to control under-actuated systems both in theoretical analysis and in practical application reviewed in [6]. Efforts [7, 8] made to design the fuzzy controllers for nonlinear overhead crane systems with input delay, actuator saturation, and dead-zone compensation and a Fuzzy-tuned PID anti-swing controller have been studied in [9].

One of the robust designs is SMC that includes switching manifold [10-13]. In [14], an overhead crane system affected by external perturbations has been controlled by a second-order sliding mode (SOSM) controller. Two control approaches of SMC with nonlinear sliding manifold and vibration strain rate feedback (SRF) have been used for flexible spacecraft attitude control in [15], and the helicopter pitch angle control problem has been simulated using an integral augmented sliding mode controller in [16].

The SMC is insensitive to variety of system uncertainties, disturbances, unknown inputs, and perturbations. This feature actually provides capability more than controller resistance and ensures asymptotic stability of the system by the Lyapunov theorem. The Fractional-Order SMC has been designed for nonlinear systems with uncertainty in [17-19]. The research [20] has controlled an isolated bridge with columns of irregular heights through a separated multilevel sliding mode controller (SMSMC) of three corresponding control signals. However, a hierarchical SMC (HSMC) can be designed by a single control signal to describe the degree of the significance of each system state variable and the reasons why it is suitable for under-actuated system [21, 22]. Also, an incremental HSMC approach has been proposed in [23]. To improve crane control performance, [24, 25] have used sliding manifold with time-varying parameters. Design of adaptive SMC is a good choice for time-varying models. In [26], an adaptive model reference with HSMC has been developed for a class of uncertain under-actuated systems with time delay and dead-zone inputs. Qian and Zou have presented an adaptive HSMC for the class of under-actuated systems in [27, 28].

The crane systems are often operated under uncertainty conditions such as un-modeled dynamics, forces, and disturbances. In this paper, the friction force is modelled as multiplicative uncertainty. Hence, SMC is designed as a robust controller in presence of uncertainties and disturbances. This system is under-actuated with two subsystems: trolley and payload. Hence, it is preferable to use combined HSMC with two-sliding manifold layers. In the first layer, the sliding manifold is defined for two subsystems. The crane model parameters are time variants such as payload mass and cable length, so adaptive control is used to adjust the behavior of the system to the desired value. In this way, the performance of the system is improved. For this reason, an ACHSMC is proposed for this system. Finally, the first layer sliding manifold parameter is calculated by GA and PSO methods to save energy of the single input of the system for each payload transferring of the crane.

This paper is organized as follows: The friction forces of the crane are modelled as multiplicative uncertainties with input signals of system in Section 2. In Section 3, the combined HSMC is defined by intermediate variables. The proposed ACHSMC is designed in Section 4, and its stability is approved and optimized by GA and PSO. Simulation results are presented and discussed in Section 5. Finally, some concluding remarks are given in Section 6.

2. Uncertainty Modeling and Problem Formulation

Fig. 1 shows the coordinate system of a single-pendulum-type crane model with its payload. Apparently, the crane system consists of two subsystems: trolley and payload. The payload is suspended from the trolley by a cable, and the system is forced by an actuating input signal which is defined in (1):

$$u = u_{act} - u_{fric} \tag{1}$$

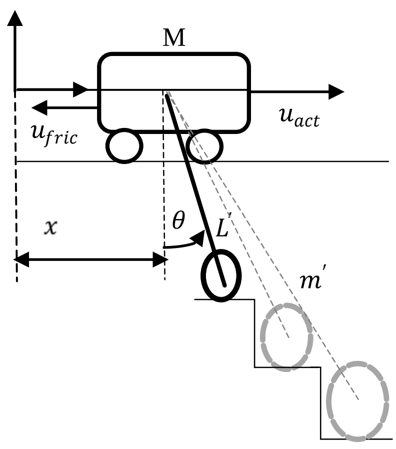

Fig. 1: The crane model with time variant load

Other symbols in Fig. 1 are described as the trolley mass M, the swing angle of the payload with respect to the vertical line θ, the trolley position x respect to the origin. $m'(t)$ and $L'(t)$ are time-varying payload mass and cable length. It is assumed that the frictional force of the system is described in (2):

[DOR: 20.1001.1.23452951.1400.11.4.1.0]

[DOI: 10.22052.11.4.2]

$$u_{fric} = (\Delta b_i)u, \qquad i = 1,2 \tag{2}$$

where the control gain Δb_i has the certain bounds, but it is unknown; it models similar to multiplicative uncertainty with input signal [11]. These boundaries are as $0 < \Delta b_{i_{\min}} \leq \Delta b_i \leq \Delta b_{i_{\max}}$ and geometric means of them is defined in (3), and original input coefficients are in (4).

$$\Delta b_i = (\Delta b_{i_{\min}} \Delta b_{i_{\max}})^{\frac{1}{2}}, \quad i = 1,2 \tag{3}$$

$$\begin{aligned} \hat{b}_1 &= \hat{b}_1(X) = \frac{1}{M + m' \sin^2 x_3} \\ \hat{b}_2 &= \hat{b}_2(X) = \frac{\cos x_3}{(M + m' \sin^2 x_3)L'} \end{aligned} \tag{4}$$

$$\begin{aligned} \dot{x}_1 &= x_2 \\ \dot{x}_2 &= f_1(X) + b_1(X)\big(u + u_{fric}\big) \\ &\qquad = f_1(X) + b_1(X)(1 + \Delta b_1)u \\ \dot{x}_3 &= x_4 \\ \dot{x}_4 &= f_2(X) + b_2(X)\big(u + u_{fric}\big) \\ &\qquad = f_2(X) + b_2(X)(1 + \Delta b_2)u \end{aligned} \tag{5}$$

The dynamic model of the crane in the state space domain is considered in (5) from [21]. Here, $x_1 = x$, $x_3 = \theta$, x_2 are the trolley velocity; x_4 is the angular velocity of the payload. The dynamics f_i have uncertainty and are not known precisely. Thus, $F_i$is additive uncertainty bound and defined as (6). Also, $\hat{f}_i$ is original model of system as (7):

$$\left|\hat{f}_i - f_i\right| \leq F_i, \quad i = 1,2 \tag{6}$$

$$\begin{aligned} \hat{f}_1(X) &= \frac{ML' x_4^2 \sin x_3 + m' g \sin x_3 \cos x_3}{M + m' \sin^2 x_3} \\ \hat{f}_2(X) &= -\frac{(M + m')g \sin x_3 + ML' x_4^2 \sin x_3 \cos x_4}{(M + m' \sin^2 x_3)L'} \end{aligned} \tag{7}$$

3. Combined Hierarchical Sliding Manifold Description

The presented crane model in [29] has four state variables as specified in (5). They can be divided into two groups. One group is composed of original x_1 and x_3 , and in the other group x_2 and x_4 are their derivatives, and e_1 and e_3 are matching errors in (8).

$$e_1 = x_1 - x_{1d}, \qquad e_3 = x_3 - x_{3d} \tag{8}$$

x_{1d} is desired trolley position, and x_{3d} is desired payload swing angle. In the first layer, we define an intermediate variable z by them as sliding manifold in (9) c is a positive constant.

$$z = e_1 + ce_3 \tag{9}$$

In the second layer, s is constructed by the intermediate variables and its derivative, which is determined by (10).

$$s = \alpha(t)z + \dot{z} \tag{10}$$

Since $m'(t)$ and $L'(t)$ are time-varying payload mass and cable length, $\alpha(t)$ is an assumed time-varying parameter and it can be positive or negative. Thus, sliding manifold s could be in any quadrant in its phase plane. The schematic of the two-layer-combined-sliding manifold is illustrated in Fig. 2. e_2 and e_4 are errors of trolley and angular velocities.

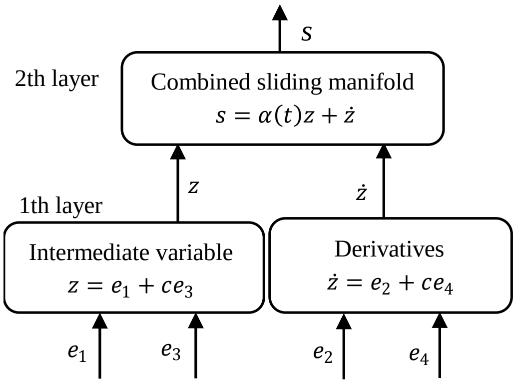

Fig. 2: Combined hierarchical sliding manifold

4. Stability Analysis and Design of ACHSMC System

For the stability of the system, a Lyapunov function candidate can be defined in (11).

$$V = 0.5\, s^2 \tag{11}$$

By using derivation of (9) and (10) and substituting (10), the derivative of Lyapunov's functions with respect to time $\dot{V}$ is described in (12).

$$\begin{aligned} \dot{V} = s\dot{s} &= s(\dot{\alpha}z + \alpha\dot{z} + \ddot{z}) \\ &= s(\dot{\alpha}z + \alpha e_2 + \alpha c e_4 + cf_2 \\ &\quad + f_1 + (b_1(1 + \Delta b_1) \\ &\quad + cb_2(1 + \Delta b_2))(u_{sw})) \end{aligned} \tag{12}$$

Now, by considering $b_{i0}(X) = b_i(X)(1 + \Delta b_i)$and $\hat{b}_{i0}(X) = b_i(X)\big(1 + \widehat{\Delta b}_i\big)$ for $i = 1,2,$ the switching control law is obtained as (13).

$$u_{sw} = -\frac{k\, sgn(s)}{\hat{b}_{10} + c\hat{b}_{20}} \tag{13}$$

The adaptive parameter $\dot{\alpha}$ is derived in Eq. (14) by an assumption $\dot{s} = 0$.

$$\dot{\alpha} = -(\|z\|^2 + \delta)^{-1}(\hat{f}_1 + c\hat{f}_2 + \alpha e_2 + \alpha c e_4 z \tag{14}$$

where δ is a small positive constant.

Equation (12) can be expressed as (15) by substituting (13) and (14).

$$\dot{V} = s(b_{10} + cb_{20}) \times \tag{15}$$

$$\left(\left(\hat{b}_{10}+c\hat{b}_{20}\right)^{-1}\left(-ksgn(s)\right)\right)$$

Thus, considering the range of k as (16), $\dot{V}$ is negative definite, and asymptotic stability of this system is approved.

$$k \geq \left(\hat{b}_{10}+c\hat{b}_{20}\right)\left(b_{10}+cb_{20}\right)^{-1}\left(F_1+cF_2\right) \quad (16)$$

5. Classical SMC Method

In this section, in order to create a comparative view, the classical sliding mode method is presented. The invariance property of sliding mode stands for the clear and significant difference between this controller and the proposed one. The classical SMC algorithm is not adaptive, and the sliding surface and control law are designed as (17) and (18) respectively.

$$s=\sum_{i=1}^{n} c_i e_i \quad (17)$$

$$u=u_{eq}+u_{sw} \quad (18)$$

which u_{eq} is equivalent control law. To obtain the equivalent control law u_{eq}, the derivative s is taken with respect to time t and the system model is substituted in it. Then, the law u_{eq} can be deduced from $\dot{s}=0$ as (19).

$$u_{eq}=-\frac{\sum_{i=1}^{n} c_{2i}\hat{f}_i+\sum_{i=1}^{n} c_{2i-1}e_{2i}}{\sum_{i=1}^{n} c_{2i}b_{i0}(X)} \quad (19)$$

The stability of this method is proved by selecting Lyapunov function candidate (11). By substituting the control law (18) and the equivalent control law (19) in the derivative V,$\dot{V}$ is achieved as (20).

$$\dot{V}=s\left(\sum_{i=1}^{n} c_{2i-1}e_{2i}+\sum_{i=1}^{n} c_{2i}f_i+\sum_{i=1}^{n} c_{2i}b_{i0}(X)\left(u_{sw}+u_{eq}\right)\right) \quad (20)$$

For the purpose of system stability, the switching law u_{sw} is defined like the ACHSMC method as in (13).

6. Energy Optimization

In this section, evolutionary algorithms GA and PSO are used to optimize the energy of the input control signal by specifying the constant variable c. In using the evolutionary algorithm to solve optimization problems, the first important task is to determine how the solution can be represented according to the elements or terminology of the specific evolutionary algorithm. The processes for initialization and generation of new population may produce infeasible solutions. It is very important to choose a solution representation that is more likely to produce feasible solutions. In addition to the solution representation, two common parameters that must be determined initially are the population size and the maximum number of iteration.

a. GA

The main idea of GA is to imitate natural selection and the survival of the fittest. In GA, solutions are ranked based on fitness values. The parents are selected based on probabilities that favor individuals with better fitness. Flow chart of genetic algorithm is shown in Fig. 3. The population size is 8 chromosomes. The crossover, mutation percentages, and the selection pressure are relatively equal to 0.8, 0.3 and 10. The GA selection method can be chosen as roulette wheel or random selection in MATLAB software.

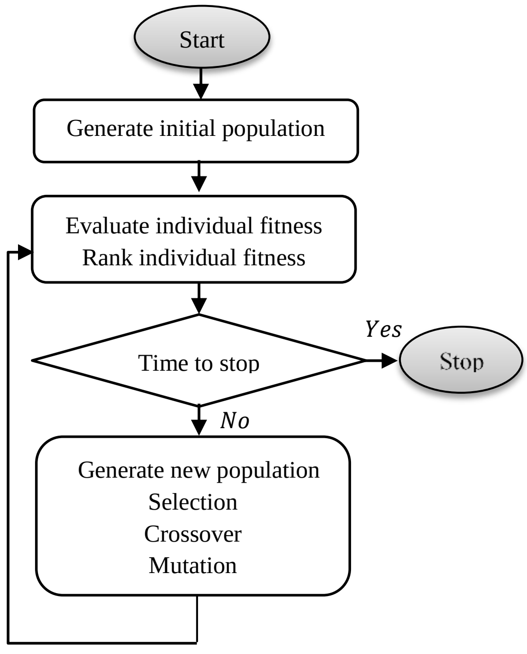

Fig. 3: Flowchart ofgenetic algorithm

b. PSO

In PSO, a solution is represented as a particle, and the population of solutions is called a swarm of particles. Each particle has two main properties: position and velocity. Each particle moves to a new position using a type of velocity. Once a new position is reached, the best position of each particle and the best position of the swarm are updated as needed. The velocity of each particle is then adjusted based on the experiences of the particle. The process is repeated until a stopping criterion is met. Flowchart of PSO is shown in Fig. 4. Initial velocity of particles is considered equal to zero. The velocity and position of each particle in the next iteration for fitness function evaluation are calculated as follows [30]:

$$x_i(t+1)=x_i(t)+v_i(t+1) \quad (21)$$

[DOR: 20.1001.1.23452951.1400.11.4.1.0]
[DOI: 10.22052.11.4.2]

$$v_i(t+1) = w[v_i(t) + \Phi_1 rand_1(P_i(t) - x_i(t)) + \Phi_2 rand_2(g(t) - x_i(t))] \quad (22)$$

$$\Phi = \Phi_1 + \Phi_1 \ . \ w = 2/(2 - \Phi - \sqrt{\Phi^2 - 4\Phi}) \quad (23)$$

The constants Φ_1 and Φ_2 are cognitive and social parameters respectively, and $rand_1$ and $rand_1$ are random values in [0, 1]. The factor Φ has an effect on the convergence characteristic of the system and must be greater than 4.0 to guarantee stability. However, as the value of Φ increases, the constriction w decreases producing the diversification which leads to slower response. The typical value of Φ is 4.1 (i.e. $\Phi_1 = \Phi_2 = 2.05$) as proposed in [31].

7. Simulation Results

The parameters of the crane model and the initial and destination state vectors are given in Table 1.

Table 1: Physical parameters of the crane

Parameters and Vectors	Value
Trolley mass M (kg)	1
Payload mass m (kg)	0.8
Cable length L (m)	0.305
Acceleration of gravity g ($\frac{m}{s^2}$)	9.81
Initial state vector x_0	$[0m \quad 0\frac{m}{s} \quad 0\,rad \quad 0\frac{rad}{s}]$
Destination state vector x_d	$[1m \quad 0\frac{m}{s} \quad 0\,rad \quad 0\frac{rad}{s}]$
additive uncertainties	$F_1 = F_2 = 2.5$
Multiplicative uncertainties	$\Delta b_1 = \Delta b_2 = 0.1$

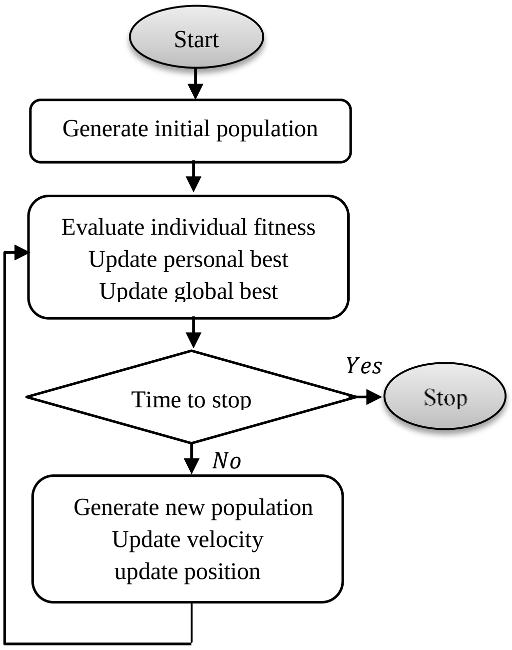

Fig. 4: Flow chart of Particle Swarm Optimization

In the classical SMC simulation, the coefficients c_i are considered equal to -3, -3, 5 and 1 in (17). Figs 5-8 show the simulation results of the proposed OACHSMC method compared to the classical SMC method.

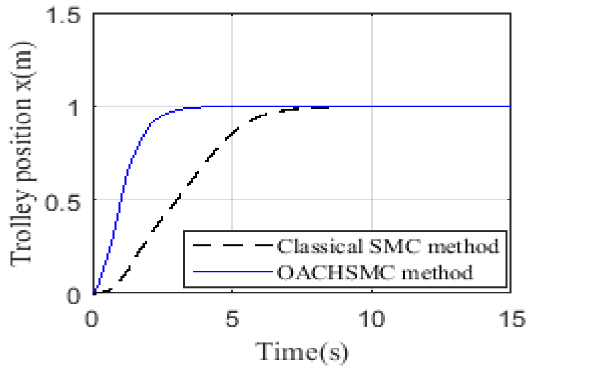

Fig. 5: Crane trolley positions

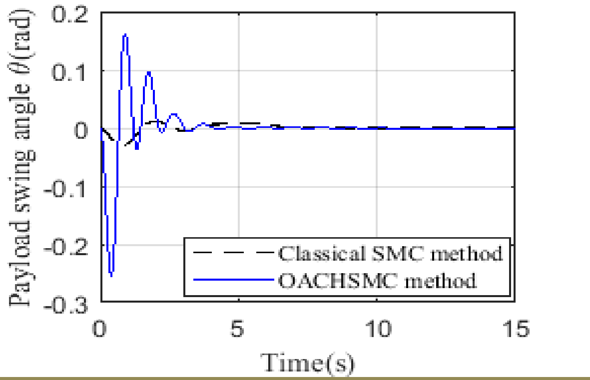

Fig. 6. Swing angle of the payload

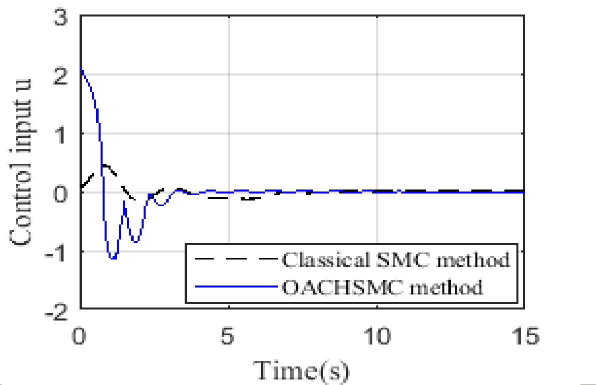

Fig. 7: Control signals

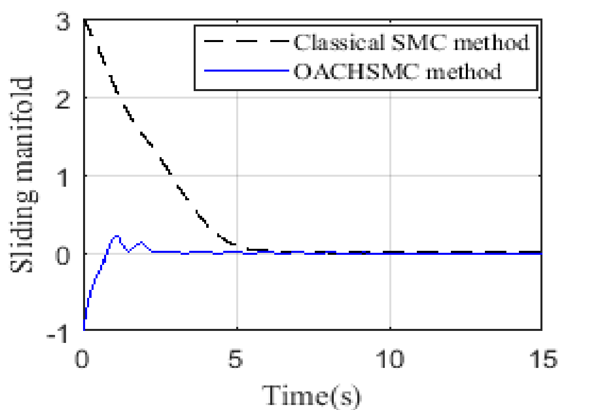

Fig. 8: Sliding manifolds

As can be seen, the convergence of the trolley position and of the payload swing angle is faster by using the proposed method. The designed OACHSMC is tested under different scenarios for time-varying payload mass and cable length during load transferring of Table 2.

Table 2: Six different scenarios for load transferring

Scenario	Time-varying Parameters	Algorithm	MaxIt.	N Pop.	Cost Function
(a)	$m' = m + \frac{2M}{T}t$	PSO	12	8	311.8913
	$L' = L = const$	GA	12	8	311.8913
(b)	$m' = m = const$	PSO	15	10	326.1994
	$L' = L(2 - \frac{1}{T}t)$	GA	15	10	326.1994
(c)	$m' = m - \frac{0.7M}{T}t$	PSO	25	15	291.5821
	$L' = L = const$	GA	25	15	291.5821
(d)	$m' = m + \frac{2M}{T}t$	PSO	18	12	315.9582
	$L' = L(1 + \frac{1}{T}t)$	GA	18	12	315.9582
(e)	$m' = m + \frac{2M}{T}t$	PSO	20	10	350.3157
	$L' = L(2 - \frac{1}{T}t)$	GA	20	10	350.3157
(f)	$m' = m - \frac{0.7M}{T}t$	PSO	20	15	317.7588
	$L' = L(2 - \frac{1}{T}t)$	GA	20	15	317.7588

The time-varying parameter $\alpha(t)$of the ACHSMC is seen in Fig. 9. Two evolutionary algorithms GA and PSO have derived the optimized value $c = 0.02$for different scenarios.

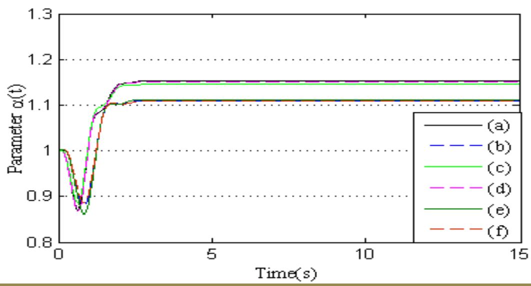

Fig. 9: Time-varying parameters$\alpha(t)$

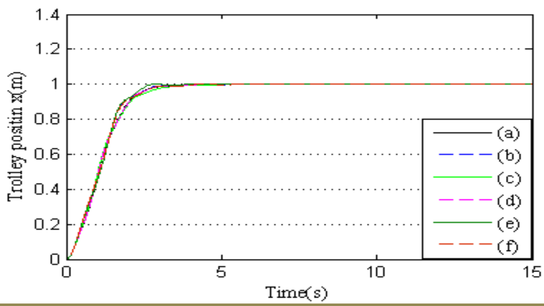

Fig. 10: Crane trolley positions

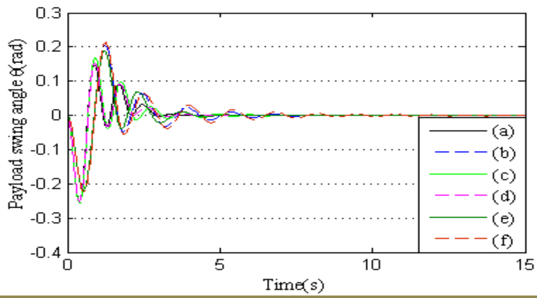

Fig. 11: Swing angle of the payload

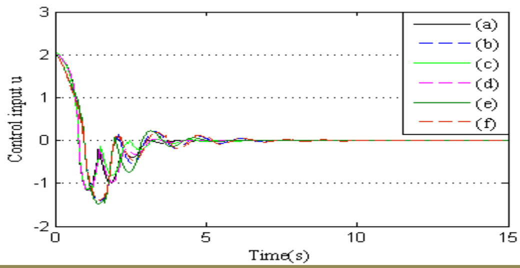

Fig. 12: Control signals

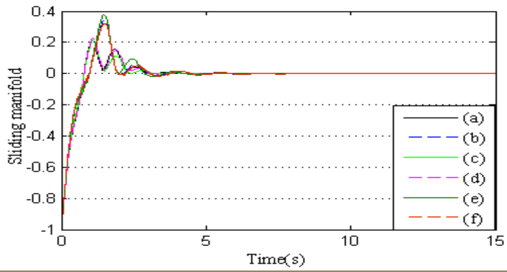

Fig. 13: Sliding manifolds

By optimization methods, the coefficient of trolley position error is selected very greater than payload angle error coefficient in (9); thus, in Figs. 10 and 11, the crane trolley reaches its destination point about 3 seconds, and payload angle deviation is damped at least in 5 seconds. Fig. 12 and 13 show the adaptive optimal input control signal u and hierarchical sliding manifold for six scenarios.

8. Conclusion

In this paper, an optimized robust controller was designed for under-actuated time-varying crane model in presence of uncertainties. The model has two subsystems with different state space variables: trolley position, payload cable angle, and their derivatives. Hence, we defined two sliding surfaces for an accurate control. In the first layer, a sliding surface was defined for original state variables and another for derivatives variables. Then, they were combined by a sliding manifold in the second layer as a hierarchical sliding mode controller. For load transferring, mass and cable length time variant was considered, and the adaptive controller was designed. For this purpose, coefficient of the second sliding manifold layer of CHSMC was adapted by time-variant variables. The stability of this controller was proven by Lyapunov theorem. Finally, to save energy of the input signal, the parameter of the first sliding manifold layer of HSMC was optimized by genetic and PSO algorithms. The proper performance and convergence of the proposed method were confirmed by comparing this method with the classical SMC method. Six different scenarios for time-varying payload mass and cable length during load transfer for crane system were simulated by MATLAB software. The results confirmed that the OACHSMC method has suitable behaviors such as optimal signal control, smooth sliding manifold, and adaptive robust stability and performance.

References

[1] Sun, N., Fang, Y., Chen, H. and Lu, B., "*Amplitude-saturated nonlinear output feedback antiswing control for underactuated cranes with double-pendulum cargo dynamics*", IEEE transactions on Industrial Electronics, Vol. 64, pp. 2135-2146, 2017.

[2] Yang, C., Li, Z., Cui, R. and Xu, B., "*Neural network-based motion control of undeactuated wheeled inverted pendulum models*", IEEE Trasactions on Neural Networks and Learning Systems, Vol. 25, pp. 2004-2016, 2014.

[3] Wang,Z. and Guo, Y., "*Unified control for pendubot at four equilibrium points*", IET Control Theory and Applications, Vol. 5, No. 1, pp. 155-163, 2011.

[4] Yang, C., Li, Z. and Li, J., "*Trajectory planning and optimized adaptive for a class of wheeled inverted pendulum vehicle models*", IEEE Transactions on Cybernetics, Vol. 43, pp. 24-36, 2013.

[5] Lai, X., Zhang, P., Wang, Y. and Wu, M., "*Position-posture control of a planar four-link underactuated manipular based on genetic algorithm*", IEEE tranactions onIndustrial Electronics, Vol. 64, pp. 4781-4791, 2017.

[6] Huang, X., Ralescu, A.L., Gao, H. and Huang, H., "*A survey on the application of fuzzy systems for underactuated systems*", Journal of Systems and Control Engineering, 2018.

[7] Zhao, Y. and Gao, H., "*Fuzzy-Model-Based Control of an Overhead Crane With Input Delay and Actuator Saturation*", IEEE Transactions on Fuzzy Systems, Vol. 20, No. 1, pp. 181–186, 2012.

[8] Chang, C.Y. and Chiang, T.C., "*Overhead cranes fuzzy control design with deadzone compensation*", Neural Computing and Applications, Vol. 18, No. 7, pp. 749–757, 2009.

[9] Solihin, M.I., Wahyudi and Legowo, A., "*Fuzzy-tuned PID anti-swing control of automatic gantry crane*", Journal of Vibration and Control, Vol. 16, No. 1, pp. 127-145, 2010.

[10] Slotin, J.J.E. and Li, W., Applied Nonlinear Control, New Jercy, 1991.

[11] Utkin, V., Guldner, J. and Shi, J., Sliding Mode Control in Electromechanical Systems, 1999.

[12] Xu, R. and Özgüner, Ü., "*Sliding mode control of a class of underactuated systems*", Automatica, Vol. 44, No. 1, pp. 233-241, 2009.

[13] Shtessel, Y., Edwards, Ch., Fridman, L. and Levant, A., Sliding Mode Control and Observation, New York, 2014.

[14] Vázquez, C., Fridman, L., Collado, J. and Castillo, I., "*Second-Order Sliding Mode Control of a Perturbed-Crane*", Journal of Dynamic Systems, Measurement, and Control, Vol. 137, No. 8, 2015.

[15] Shahravi, M. and Azimi, M., "*A Hybrid Scheme of Synthesized Sliding Mode/Strain Rate Feedback Control Design for Flexible Spacecraft Attitude Maneuver Using Time Scale Decomposition*", Int. J. Structural Stability and Dynamics, Vol. 16, pp. 1450101, 2016.

[16] Zaeri, A.H., Noor, S.B.M., Isa, M.M. and Taip, F.S., "*Design of Integral Augmented Sliding Mode Control for Pitch Angle of a 3-DOF Bench-top Helicopter*", Majlesi Journal of Electrical Engineering , Vol. 4, No. 3, pp. 31-35, 2010.

[17] Fei, J. and Wang, H., "*Recurrent Neural Network Fractional-order Sliding Mode Control of Dynamic Systems*", Journal of the Franklin Institute, pp. 1-20, 2020.

[18] Hashtarkhani, B. and Khosrowjerdi, M.J., "*Adaptive actuator failure compensation for uncertain nonlinear fractional order strict feedback form systems*", Trans. of the Institute of Measurement and Control, Vol. 41, No. 4, pp. 1032-1044, 2019.

[19] Fei, J. and Lu, C., "*Adaptive Fractional Order Sliding Mode Controller with Neural Estimator*", Journal of the Franklin Institute-engineering and Applied Mathematics, Vol. 355, No. 5, pp. 2369-2391, 2019.

[20] Lee, T.Y., Chen, P.C. and Juang, D.S., "*Sliding mode control on isolated bridges with columns of irregular heights using pole assignment and PSO-SA hybrid algorithm*", Int. J. Structural Stability and Dynamics, Vol. 12. No. 3, pp. 1250014, 2012.

[21] Qian, D. and Yi, J., Hierarchical Sliding Mode Control for Underactuated Cranes, 2016.

[22] Shin, S.Y. and Lee, J.J., "*Fuzzy sliding mode control for an under-actuated system with mismatched uncertainties*", Artificial Life and Robotics, Vol. 15, No. 3, pp. 355–358, 2010.

[23] Mazinan, H., Ebrahimi Mollabashi, A.H., "*Incremental SMC-based CNF control strategy considering magnetic ball suspension and inverted pendulum systems through*

[DOR: 20.1001.1.23452951.1400.11.4.1.0]

[DOI: 10.22052.11.4.2]

cuckoo search-genetic optimization algorithm", Complex & Intelligent Systems, Vol. 5, pp. 353–362, 2019.

[24] Choi, S., Park, D. and Jayasuriy, S., "*A time-varying sliding surface for fast and robust tracking control of second-order uncertain systems*", Automatica, Vol. 30, No. 5, pp. 899–904, 1994.

[25] Tavanaei Sereshki, Z., Pariz, N. and Kardan, I., "*New Adaptive Sliding Mode Controller for Depth Control of Autonomous Underwater Robot*", Majlesi Journal of Electrical Engineering, Vol. 9, No. 3, pp. 1-6, 2015.

[26] Chiang, C.C. and Chen, Y.C., "*Adaptive Model Reference Hierarchical Sliding Mode Control of Uncertain Underactuated System with Time Delay and Dead-Zone Input*", International Journal of Control Science and Engineering, Vol. 9, No. 1, pp. 15-25, 2019.

[27] Qian, D., Liu, X., Yi, J., "*Adaptive Control Based on Incremental Hierarchical Sliding Mode for Overhead Crane Systems*", Applied Mathematics & Information Sciences, Vol. 7, No. 4, pp. 1359-1364, 2013.

[28] Zou, Y., "*Nonlinear robust adaptive hierarchical sliding mode control approach for quadrotor*", Int. J. of Robust Nonlinear Control, 2016.

[29] Qian, D. and Yi, J., "*Design of combining sliding mode controller for overhead crane systems*", Int J Control Autom, Vol. 6, No. 1, pp. 131–140, 2013.